Variation in the distribution of Yellowfin Sole *Limanda aspera* larvae in warm and cold years in the eastern Bering Sea

Steven M. Porter

Correspondence
Steven M. Porter, Recruitment Processes Program, Resource Assessment and Conservation Engineering Division, Alaska Fisheries Science Center, NOAA, National Marine Fisheries Service, 7600 Sand Point Way NE, Seattle, Washington 98115, USA
Email: steve.porter@noaa.gov

Abstract

Multi-year periods of relatively cold temperatures (2007-2013), and warm temperatures (2001-2005 and 2014-2018) altered the eastern Bering Sea ecosystem, affecting ocean currents and wind patterns, plankton community, and spatial distribution of fishes. Yellowfin Sole *Limanda aspera* larvae were collected from the inner domain (≤ 50 m depth) of the eastern Bering Sea among four warm years (2002, 2004, 2005, 2016), an average year (2006), and three cold years (2007, 2010, 2012). Spatial distribution and density of larvae among those years was analyzed using generalized additive models that included timing of sea-ice retreat, areal coverage of water ≤ 0° C, and water temperature as covariates. Analyses indicated a combination of temperature effects on the location and timing of spawning, and on egg and larval survival may explain the variation in larval density and distribution among years. During warm years, higher density and wider spatial distribution of larvae may be due to earlier spawning, an expansion of the spawning area, and higher egg and larvae survival due to favorable temperatures. Larval distribution contracted shoreward and density was lower during cold conditions, and was likely due to fish spawning closer to shore to remain in preferred temperatures, later spawning, and increased mortality. Predicted drift trajectories from spawning areas showed that larvae would reach nursery grounds in most years. Years when the drift period was longer than the pelagic phase of the larvae occurred during both warm and cold conditions indicating that settlement outside of nursery areas could happen during either temperature condition.

47 1. INTRODUCTION

48 The larval stage of flatfishes connects spawning area to juvenile nurseries. Changes in
49 spawning location may affect the ability of larvae to reach nursery areas, and flatfish larvae must
50 reach suitable benthic habitat for settlement and continued growth and development (Duffy-
51 Anderson et al., 2015). Flatfish larvae are planktonic, offshore spawning flatfish species use
52 currents to transport larvae to nursery areas and nearshore spawning species rely on retention
53 features to maintain larvae near nursery areas (Duffy-Anderson et al., 2015). Juvenile flatfishes
54 have specific habitat preferences (e.g., sediment grain size and temperature; Duffy-Anderson et
55 al., 2015) and success in reaching nurseries may play a role in recruitment variability in flatfishes
56 (Bailey et. al, 2008). Multi-year periods of warm and cold temperature conditions observed in
57 the southeastern Bering Sea from 2001 to 2018 (Stabeno and Bell, 2019) affected the extent of
58 flatfish spawning habitat (e.g., Porter and Ciannelli, 2018) and accessibility to their nursery areas
59 (e.g., Cooper et al., 2014). For example, the spawning area of Flathead Sole *Hippoglossoides*
60 *elassodon* expanded during warm conditions (Porter and Ciannelli, 2018). The transport patterns
61 of Northern Rock Sole *Lepidopsetta polyxystra* larvae to a northern nursery area varied due to
62 differences in the direction of near-surface currents between warm and cold years (Cooper et al.,
63 2014). Larvae were transported to that nursery in warm years and in cold years larvae were
64 transported offshore (Cooper et al., 2014).

65 The eastern Being Sea shelf is divided at ~60° N latitude into northern and southern regions
66 based on differences in the physical oceanographic properties and biology of the two areas. In
67 the northern region, sea-ice arrives earlier and persists longer than in the south, shelf water is
68 colder and relatively fresh, and a predominantly benthic food web occurs there (Stabeno et al.,
69 2010; Stabeno et al., 2012a). The southern region is warmer and saltier, and primarily supports a
70 pelagic food web (Stabeno et al., 2010; Stabeno et al., 2012a). Temperature conditions in the

eastern Bering Sea can vary interannually or persist through multi-year periods of warm or cold conditions. The northern region had no trend in the timing of the arrival, duration, or retreat of sea-ice in years prior to 2015, but in 3 out of the 4 years from 2014 to 2018, ice formed later and melted earlier there than previous years (Stabeno et al., 2019). Winter sea-ice coverage in the southern region is more variable than in the northern region (Stabeno and Bell, 2019). Prior to 2000 the interannual variability of the extent of sea-ice on southeastern Bering Sea shelf was high (Stabeno et al., 2012b). Beginning in 2001 the shelf alternated between multi-year periods of warm (2001-2005, 2014-2018) and cold (2007-2013) conditions (stanzas) during the spring, summer and fall (Stabeno et al., 2012b). Major characteristics of warm years are relatively low areal sea-ice extent, winds out of the south, and near surface current direction is variable and relatively weak (Stabeno et al., 2012b). Cold years are characterized by high sea ice extent, winds out of the northwest, and near surface currents have a significant westward component (Stabeno et al., 2012b). The stanzas altered the ecosystem, affecting ocean currents and wind patterns, zooplankton types and abundance, and spatial distribution of fishes (Stabeno et al., 2012b; Barbeaux and Hollowed, 2018; Stabeno and Bell, 2019). On the southeastern Bering Sea shelf, water from melting sea-ice mixes in the water column to create a bottom layer of cold water 40 to 50 m thick in the middle domain (50 to 100 m depth, Fig. 1) that persists in the late spring and summer (called the "cold pool", identified by water temperatures $< 2°$ C; Stabeno et al., 2001). The spatial extent of the cold pool varies interannually depending on the coverage of winter sea-ice. In warm years the extent of the cold pool is limited farther north than in cold years, when it can extend southward down the middle domain as far as the Alaska Peninsula (Kotwicki and Lauth, 2013).

93 Yellowfin Sole (YFS) *Limanda aspera* are one of the most abundant flatfish species in the
94 eastern Bering Sea and are the basis for the largest flatfish fishery in the world (Spies et al.,
95 2019). The fishery occurs year round, and the largest catches occur in spring and early summer,
96 and late summer and early fall (Spies et al, 2020). Commercial fishing mostly occurs in the
97 middle and inner (≤ 50 m depth) domains of southeastern Bering Sea shelf (Spies et al, 2020;
98 Fig. 1). In 2018, the commercial catch totaled more than 280 million pounds with a value of
99 more than $60 million (Retrieved June 2021 from
100 https://www.fisheries.noaa.gov/species/yellowfin-sole#overview). Beginning in April or early
101 May as the sea-ice edge recedes and temperatures warm, YFS migrate eastward from wintering
102 grounds located west of the Pribilof Islands near the shelf break (approximately 200 m depth)
103 and near Unimak Island (Wakabayashi, 1989) to nearshore waters (inner domain) of the Alaska
104 coast for feeding and spawning (Wilderbuer et al., 2018; Fig. 1). Based on tagging studies, the
105 Pribilof Island group migrates to areas north and south of Nunivak Island, and the Unimak Island
106 group migrates to those same areas and additionally to Bristol Bay (Wakabayashi, 1989; Fig. 1).
107 Spawning occurs from Bristol Bay to near St. Lawrence Island (Bakkala, 1981) from mid-May
108 through August and possibly into September (Waldron, 1981). The majority of spawning takes
109 place in depths < 30 m (Nichol, 1995), and may occur as deep as 50 m (Wakabayashi, 1989).
110 YFS eggs are pelagic (Matarese et al., 2003), they are spawned in an uninterrupted succession of
111 batches, and adults remain in the spawning area until they are spent and then move to deeper
112 water (Nichol and Acuna, 2001). YFS may be able to spawn more than one series of batches
113 within a single year (Nichol and Acuna, 2001). Egg abundance determined from ichthyoplankton
114 surveys indicate that spawning is most intense south and southeast of Nunivak Island (Bakkala,
115 1981). For a closely related species, Yellowtail Flounder *Limanda ferrunginea* found along the

116 Atlantic coast of North America (Cooper and Chapleau, 1998), time from fertilization to 50%
117 hatching was about 6 days at 8° C (Laurence and Howell, 1981). Pelagic phase of YFS larvae
118 varies between 30 and 60 days (Duffy-Anderson et al., 2015).
119 YFS spawn nearshore so oceanographic retention features are crucial to keep larvae near their
120 nursery areas (Duffy-Anderson et al., 2015). Weak currents (Kinder and Schumacher, 1981;
121 Stabeno et al., 2016) and a front located near the 50 m isobath (Coachman, 1986) are
122 oceanographic features that may help to retain YFS larvae in the inner domain. Juvenile YFS
123 inhabit the inner domain of the southeastern Bering Sea, ranging from Bristol Bay to Nunivak
124 Island (Bartolino et al., 2011; Yeung and Yang, 2017; Yeung and Yang, 2018), and are known to
125 be concentrated near Kuskokwim and Togiak Bays (Spies et al., 2019; Fig. 1). Norton Sound
126 may be a nursery area in the northern Bering Sea (Spies et al., 2019; Fig. 1). Larvae reaching
127 those areas for settlement is crucial for growth and survival of juveniles.
128 Temperature is an important factor affecting the timing of spawning and spatial distribution
129 of YFS in the eastern Bering Sea (Bartolino et al., 2011; Nichol et al., 2019), and therefore can
130 also affect the spatial distribution and abundance of YFS larvae. YFS spawning occurred earlier
131 during warm years as evidenced by an increase in spent females in water deeper than 50 m
132 during those years (Nichol et al., 2019). Sea-ice edge retreat can affect the timing of YFS
133 spawning because YFS follow the receding ice edge in their migration eastward in the spring
134 (Bakkala, 1981). Bottom trawl surveys conducted during warm, intermediate, and cold
135 temperature conditions indicated that the rate of migration to more northern waters of their
136 spawning area may be slower in cold years than in warm years (Bakkala, 1981). Adults avoid
137 temperatures colder than 0° C and their distribution expands northward as temperatures warm
138 and the cold pool contracts (Bartolino et al., 2011).

139 The objective of this study was to evaluate the effects of timing of sea-ice retreat, areal
140 coverage of water colder ≤ 0° C, and water temperature on the distribution and abundance of
141 YFS larvae in the inner domain of the eastern Bering Sea from ichthyoplankton surveys, and use
142 generalized additive models to assess how warm and cold years affected larval distribution.
143 Additionally, to relate how differences in environmental conditions among years could affect
144 larvae access to nursery areas. This study was limited to the inner domain because most YFS
145 spawning occurs within that domain (Nichol, 1995), and YFS nursery areas are located there
146 (Bartolino et al., 2011; Yeung and Yang, 2017; Yeung and Yang, 2018, Spies et al., 2019).
147 Differences in larval abundance and distribution within that domain among years could be the
148 result of shifts in the location or timing of spawning, changes in larval drift due to environmental
149 conditions, and temperature effects on larval survival. Location and timing of spawning are
150 thought to be connected to environmental conditions beneficial for early life survival such as
151 dispersal of larvae into favorable habitats, and overlap of larvae and their prey (Leggett, 1985;
152 Ciannelli et al., 2015), so any changes in timing or location can potentially have consequences on
153 early life survival and recruitment.
154
155 ## 2. MATERIALS AND METHODS
156 ### 2.1 Larvae collections
157 YFS larvae were collected using a 60-cm bongo frame fitted with 505-µm mesh nets towed
158 obliquely to a maximum depth of 300 m or 10 m off bottom, whichever was shallower during
159 ichthyoplankton surveys conducted in the eastern Bering Sea by the NOAA, Alaska Fisheries
160 Science Center (AFSC; Matarese et al., 2003). The depth range for YFS larvae in the Bering Sea
161 is unknown, but larvae of Yellowtail Flounder are most abundant at 20 m depth during the day

and near the surface at night (Smith et al., 1978). Northern Rock Sole *Lepidopsetta polyxystra* larvae in the Bering Sea also show a similar vertical distribution, these larvae are near surface at night (0-10m) and in the upper 30 m during the day (Lanksbury et al., 2007). If YFS larvae have a similar vertical distribution as those species, then the net tows should have collected most of the YFS larvae in the water column. Water temperature was measured using a Sea-Bird SBE 19 SeaCat or SBE 39 FastCat CTD profiler attached to the towing wire, or from CTD casts. Ichthyoplankton samples were preserved in 5% formalin, and then larvae were sorted and identified to species at the Plankton Sorting and Identification Center in Szczecin, Poland (Matarese et al., 2003). The number of larvae caught was standardized to number/10 m^2 based on net mouth area, tow depth, and tow duration (here after referred to as density; Matarese et al., 2003), and data were retrieved from NOAA, AFSC ECODAAT ichthyoplankton database (Retrieved May 2018 from http://ecodaat.afsc.noaa.gov/). Larvae were sampled from a systematic grid design of fixed locations (Fig. 2). Years 2002, 2004-2007, 2010, 2012, and 2016 were chosen because for those years the inner domain was consistently sampled so that areal coverage was similar (Fig. 2). Depth-averaged temperature measured at a mooring located near the center of the southeastern Bering Sea shelf (middle domain; Fig. 1) was used to classify water temperature conditions for the spring, summer, and fall in that region (warmer than average, colder than average, or average, here-after referred to as warm, cold or average; Stabeno et al., 2012b). Two warm periods (2001-2005, and 2014-2016), one cold period from 2007-2013, and an average year (2006) were included in the years examined in this study (Stabeno and Bell, 2019). Temporal coverage varied by year and encompassed May through early October (Table 1). For years examined in this study, only one station was occupied in June, and no sampling was

conducted in July. August and September were in common to all years. The YFS spawning season is believed to be mid-May through August and possibly into September (Waldron, 1981).

Bottom water temperatures were measured during the annual AFSC summer eastern Bering Sea bottom trawl surveys that began in early June and finished near the end of July or early August. Temperatures were contoured using the Inverse Distance Weighted function in ArcMap 10.7 (ESRI Inc., 2018).

2.2 Generalized additive models

Generalized additive models (GAM) were used to analyze the spatial distribution and abundance of YFS larvae among years. Covariates included in GAMs were near bottom temperature (t; measured approximately 10 m off bottom from a bongo net tow or CTD cast), location of a net tow (latitude (ϕ) and longitude (λ)), Julian day (d) to account for differences in larval density due to survey date, year (yr), ice retreat index (IRI), and ratio of area covered by bottom water $\leq 0°$ C to total bottom trawl survey area (RA0C). Location (latitude and longitude) and depth on the eastern Bering Sea shelf are correlated because shelf bathymetry is relatively flat with maximum depth at the shelf break (Stabeno et al. 2016), so any depth effect on larval density was accounted for by latitude and longitude in the models tested. Year was used as a factor, therefore affecting the model intercept. Sea-ice coverage and cold pool extent can vary greatly between warm and cold years and are indicative of temperature conditions. Extensive sea-ice, late sea-ice retreat, and cold pool extending far south in the middle domain are characteristics of a cold year. Ice retreat index (IRI, retrieved November 2018 from www.beringclimate.noaa.gov) is defined as the number of days after March 15 that the average sea-ice concentration within a 2° x 2° box centered on a mooring located on the southeastern Bering Sea shelf (Fig. 1) is > 10% of the total box area. IRI was included because YFS may

follow the receding sea-ice edge during their eastward cross-shelf migration in the spring (Bakkala, 1981) and this index could give an indication as to the relative timing of the arrival of YFS adults to the inner domain. IRI also is indicative of temperature conditions, in that a later ice retreat is associated with cold conditions. Ratio of area covered by bottom water ≤ 0° C to bottom trawl survey area (RA0C) represented the spatial extent of the portion of the cold pool with bottom water ≤ 0° C. The ratio is based on the total area covered by the AFSC summer bottom trawl survey on the southeastern Bering Sea shelf. The spatial extent of water ≤ 0° C could alter YFS cross-shelf migration because adults avoid bottom water temperatures colder than 0° C (Bartolino et al., 2011). Changes in migration pattern may affect spawning location and therefore alter the spatial distribution and abundance of larvae.

Given the overdispersed nature of the data set (49% of the tows did not catch YFS larvae; see Table 1 for variability of larvae density by year) a two-step approach to analyze and predict the distribution of larvae was used (Fox et al., 2000). Both a binomial presence-absence model with a logit link function, and a positive abundance model with lognormal distribution family (i.e., a model using only tows with natural log transformed larval density > 0 as the response variable) were formulated. The presence-absence model predicted the probability that YFS larvae were present, and the positive abundance model predicted density of larvae. Spatially invariant and spatially variable coefficient models (Bacheler et al., 2009) were formulated for both presence-absence and positive abundance models. In the spatially invariant models the effects of near bottom temperature, IRI, and RA0C can equally apply to all locations sampled and can be non-linear:

$$logit(\mu_i) = a_{yr} + s_1(t_{\phi,\lambda,yr}) + s_2(\phi, \lambda) + s_3(d) + s_4(IRI_{,yr}) + s_5(RA0C_{,yr}) \quad (1)$$

and

$$\ln(x_{yr,\,t,\,\phi,\,\lambda,d,IRI,RA0C}) = a_{yr} + s_1(t_{\phi,\,\lambda,\,yr}) + s_2(\phi,\,\lambda) + s_3(d) + s_4(IRI_{yr}) + s_5(RA0C_{yr}) + \mathcal{E}_{yr,\,d,\,t,\,\phi,\,\lambda,IRI,RA0C}, \quad (2)$$

where μ_i is the probability of YFS larvae being present in the i^{th} sample, x is the local YFS larvae density, a is the model intercept that varies according to year (subscript yr), s_n are nonparametric smoothing functions and $\mathcal{E}$ is the error term. In the spatially variable coefficient models the effects of IRI and RA0C were spatially variable, that is locally linear, but smoothly changing over space:

$$logit(\mu_i) = a_{yr} + s_1(t_{\phi,\,\lambda,\,yr}) + s_2(\phi,\,\lambda) + s_3(d) + s_4(\phi,\,\lambda)IRI_{yr} + s_5(\phi,\,\lambda)RA0C_{yr} \quad (3)$$

and

$$\ln(x_{yr,\,t,\,\phi,\,\lambda,d,IRI,RA0C}) = a_{yr} + s_1(t_{\phi,\,\lambda,\,yr}) + s_2(\phi,\,\lambda) + s_3(d) + s_4(\phi,\,\lambda)IRI_{yr} + s_5(\phi,\,\lambda)RA0C_{yr} + \mathcal{E}_{yr,\,d,\,t,\,\phi,\,\lambda,IRI,RA0C}. \quad (4)$$

Variable selection for each model was based on Akaike Information Criterion (AIC) using a backward stepwise process. AIC is a measure of the model goodness of fit (negative log-likelihood) penalized by the model number of parameters. AIC score was also used to select the formulation (i.e., spatially invariant or spatially variable coefficient model) for the presence/absence and abundance models that were most supported by the data. Residuals for each model were visually assessed to check for normality and independence. All models were run in R version 3.6.1 (R Core Team, 2019) using the *mgcv* package (version 1.8-28; Wood, 2006).

The predicted larval density at each location was the product of the predicted values from the best-fit presence-absence and positive abundance models. An advantage of the two-step approach is that it takes into account the possibility that there are different processes affecting the presence and density of larvae (Potts and Elith, 2006); that is, there can be different covariate effects in each model. Contour plots of predicted larval density were made using the Inverse Distance Weighted option in ArcMap 10.7 (ESRI Inc., 2018).

253 2.3 Egg collections

254 To investigate whether variability in larval distribution between warm and cold conditions
255 could be related to changes in spawning location, egg data were used as a proxy for spawning
256 location. Distribution of eggs by bottom depth within the study area was used to indicate where
257 spawning was occurring to assist with the interpretation of the predicted distribution of larvae.
258 Eggs were collected from the same surveys that collected larvae, and abundance (number/10 m^2)
259 was determined using the same methods described for larvae. Eggs were identified to genus
260 (*Limanda* sp.), and they were most likely YFS (*Limanda aspera*) because eggs were collected
261 from known YFS spawning areas during the spawning season, this species is one of the most
262 abundant flatfish species in the eastern Bering Sea (Wilderbuer et al., 2018), and eggs are pelagic
263 (Matarese et al., 2003). Positive egg abundance (> 0) from August and September in the southern
264 region of the study area was examined because those months were common to all years of this
265 study. The southern region of the study area was divided into three bottom depth intervals: < 30
266 m, 30 - 39 m, and 40-50 m. Years were grouped into cold (2007, 2010, 2012) and not-cold
267 (2002, 2004-2006, 2016) temperature categories because the shallowest bottom depth interval
268 was not sampled all years. An ANOVA using bottom depth interval and temperature category as
269 factors, and natural log transformed egg abundances as the dependent variable was run to
270 examine differences in egg abundance with depth. ANOVA and the Tukey HSD multiple
271 comparison test were run in R version 3.6.1 (R Core Team, 2019).

272 2.4 Larval drift

273 The Ocean Surface Currents Simulations (OSCURS) model
274 (oceanview.pfeg.noaa.gov/oscurs) that calculates water movement in the near-surface mixed
275 layer was used to examine YFS larvae drift during the spawning season for each year from three

known spawning areas that are indicated in Figure 16 from Wakabayashi, 1989. OSCURS calculates daily ocean surface currents anywhere in a 90-km ocean-wide grid from Baja California to China and from 10° N to the Bering Strait using daily sea level pressure (oceanview.pfeg.noaa.gov/oscurs). This model was appropriate to use for examining drift of YFS larvae because larvae may be most abundant within 20 to 30 m of the surface during the day and near the surface at night if their vertical distribution is similar to Yellowtail Flounder larvae (Smith et al., 1978) and Northern Rock Sole (Lanksbury et al., 2007). The same starting location within each spawning area was used for all years so that the ending location would only be due to winds during that year, and not be confounded with starting location. Starting point was located near the center of each spawning area and at < 30 m bottom depth because larvae would be expected to occur in high density there during both warm and cold conditions. Drift trajectories for each year began June 1 and ended October 6, the latest day of this study (126 days later). June 1 was chosen as the starting date because it is near the beginning of the YFS spawning season, and the study area was mostly free of sea-ice beginning that month for all years (Historical Sea Ice Atlas, University of Alaska. 2020. Retrieved June 2020 from http://seaiceatlas.snap.uaf.edu/).

3. RESULTS

3.1 Presence-absence and positive abundance models

The presence-absence model that best fit the data included near bottom temperature, location, day, year, and spatially variable effect of IRI (Table 2, equation 3). Presence of YFS larvae increased to about day 200 (late July; Fig. 3a). YFS spawn during late spring and summer (Nichol, 1995) and the increase in the probability of larval presence during that time is most

likely due to increased spawning activity. Larvae were most likely to be present from Bristol Bay to Norton Sound (Fig. 3b), areas that include known YFS spawning areas (Bristol Bay, and north and south of Nunivak Island; Wakabayashi, 1989). The probability of larvae being present increased in an easterly direction (that is, as depth became shallower; Fig. 3b). The majority of spawning takes place in depths < 30 m (Nichol, 1995), this can account for the increase in larvae presence toward shore. Probability of larvae being present increased as near bottom temperature warmed to 10° C, and for temperatures warmer than 10° C the probability decreased suggesting that larvae may have reached a thermal limit (Fig. 3c). The spatially variable effect of IRI showed the highest probability of presence was in the northwest region (Fig. 3d). This may be the result of the timing of sampling and delayed spawning due to cold conditions. Based on median sampling date, sampling in the southern region (< 60° N) was about one month earlier than in the northern region for most years (except for 2006 and 2016; Table 1). If spawning were delayed due to cold conditions, there would be fewer larvae present in the southern region one month earlier than when the northern region was sampled. There was no trend for the partial effect of year with respect to warm and cold conditions. Most years showed either no effect or a negative on presence, the exceptions were two warm years (2004 and 2016) that positively affected presence (Fig. 3e).

The model that best fit the density of larvae included near bottom temperature, location, day, year, spatially variable IRI, and spatially variable RA0C (Table 2, equation 4). Peak larval density occurred about day 220 (early August; Fig. 4a). Highest density occurred between Bristol Bay and Nunivak Island (Fig. 4b). Density increased as near bottom temperature warmed to about 10°C similar to the presence/absence model (Fig. 4c). The spatially variable effect of IRI showed an increase in density nearshore, suggesting that as ice retreated later in the spring

(indicating cold conditions), larvae tended to be distributed closer to shore (Fig. 4d). The spatially variable effect of RA0C indicated an increase in density in the northern region (Fig. 4e), and that may be the result of the timing of sampling and delayed spawning due to cold conditions, as described for the presence/absence model. Generally, warm years showed a positive effect on density, and cold years (2010 and 2012, the coldest years of this study; Stabeno et al., 2017) had a negative effect on density (Fig. 4f).

3.2 Predicted larval density

Predicted larval density from mid-August through September/early October was examined because this time period was in common to all years and covered the entire study area each year. Distribution and density of larvae in the southern region was more variable than the northern region (Fig. 5). In the northern region, the highest density of larvae was consistently between the 30 m isobath and the coastline, and density decreased during cold conditions (Fig. 5). In the southern region during warm years the density of larvae was highest and they were distributed throughout this region (2002, 2004, 2005, 2016; Fig. 5a, b, c, h). The extent of water $\leq 0°$ C was northern most and smallest during that time (Table 1, Fig. 6a, b, c, h). As the area of 0° C water became larger and extended southward (indicating colder conditions, Fig. 6d, e, f, g), the density of larvae between the 30 m and 50 m isobaths in the southern region decreased, and highest density was located between 30 m depth and the coastline showing a shift in density shoreward (Fig. 5d, e, f, g). Density of larvae in the southern region was lowest during the two coldest years (2010 and 2012; Fig. 5f, g). The effect of cold conditions was not as apparent for 2007 (Fig. 5e) possibly because this was the first year of the cold stanza and it takes two or more consecutive cold years for effects to become clear (Stabeno et al., 2017). A mismatch between survey timing

and larvae because of delayed spawning during cold conditions could have also contributed to differences in larval density between warm and cold years.

3.3 Distribution of eggs

Egg abundance varied with bottom depth between warm and cold conditions as indicated by a significant interaction between bottom depth interval and temperature category (ANOVA, $F_{2,170} = 5.59$, $p = 0.004$). During cold conditions, eggs were significantly more abundant in the shallowest bottom depth interval (< 30 m) compared to the deepest interval (40 – 50 m; Tukey HSD multiple comparison test, $p = 0.008$; Fig. 7). Egg abundance in the intermediate bottom depth interval (30 - 39 m) was also significantly larger than deepest interval ($p = 0.02$; Fig. 7). Abundance was not significantly different between the shallowest and intermediate intervals ($p = 0.52$; Fig. 7) even though the difference in mean egg abundance between those intervals (1258.29 eggs/10 m^2) was larger than the difference between the intermediate and deepest intervals that were significantly different (652.44 eggs/10 m^2). The lack of a significant difference between the shallowest and intermediate intervals could be due to low statistical power because of small sample size for the shallowest interval ($n = 4$; $n = 20$ and 31 for the intermediate and deepest intervals respectively). During cold conditions egg abundance most likely was highest in the shallowest bottom depth interval (< 30 m depth) suggesting that adults stayed near the coastline to spawn where warmest temperatures were located (Fig. 6e, f, g; Fig. 7), and that coincides with where larval density was highest (Figs. 5e, f, g). Egg abundance was not significantly different among bottom depth intervals for not-cold conditions (Tukey HSD multiple comparison test, $p > 0.98$; Fig. 7) suggesting that spawning was spread across the southern area during warm and average conditions, and this is consistent with the predicted larval distribution.

3.4 Drift

Drift of larvae out of the study area was most likely minimal because almost all trajectories ended within the inner domain (Fig. 8). Drift trajectories from June to October mostly followed wind patterns typical of warm and cold years, that is, winds out of the north during cold years, and from the south during warm years (Stabeno et al. 2012a). Drift from spawning sites during the cold years 2007 and 2012 was southward (Fig. 8a, b, c), and drift in 2010 began as southward and then reversed direction to northward indicating that wind had changed direction (Fig. 8a, b, c). Direction of drift during average or warm conditions was variable. Drift trajectories ranged from to the north, northeast, or northwest as would be expected for warm conditions (Stabeno et al. 2012a), but also could be to the south, or southeast depending on the year (Fig. 8d, e, f). For most years, drift trajectories from the three spawning areas showed that larvae could reach known or hypothesized YFS nursery areas (Norton Sound, Kuskokwim Bay, Togiak Bay, and Bristol Bay; Yeung and Yang, 2018; Spies et al., 2019; Fig. 8).

Bristol Bay spawning area

For all years, drift from this spawning area ended in or near known or hypothesized nursery areas. In years 2002, 2004, and 2005, drift trajectories were to the northwest toward the southern side of Cape Newenham or to Hagemeister Island (Fig. 8d). Those locations are near Togiak Bay that is thought to be a YFS nursery area (Fig.1; Spies et al., 2019). Drift in 2010 was to the north toward Togiak Bay, but rather than a direct route as in warm years (2002, 2004, and 2005), drift started to the southwest away from the coastline and then reversed direction heading toward the coast indicating that wind direction had changed during the drift period (Fig. 8a). Drift was to the southeast across Bristol Bay to the Alaska Peninsula for years 2006, 2007, 2012, and 2016 (Fig. 8a, d), and in those years drift was the longest duration to reach the coastline among all years

(Table 3). The duration of drift in 2006 and 2016 (66 days and 42 days, respectively, Table 3) showed that larvae may not have reached nursery areas at the end of their pelagic phase because the pelagic phase of YFS larvae may last 30 to 60 days (Duffy-Anderson et al., 2015).

Spawning area south of Nunivak Island

Drift from this spawning area ended near or inside Kuskokwim Bay (2005, 2007, 2012, and 2016), at the southern end of Nunivak Island (2002, 2004, and 2010), or did not reach a nursery area (2006; Fig. 8b, e). Drift trajectories showed that larvae could remain in the area between Cape Newenham and Nunivak Island near Kuskokwim Bay where juvenile YFS are found (Bartolino et al., 2011; Yeung and Yang, 2017). For the years 2004, 2005, and 2006, the period of time spent drifting towards nursery areas was considerable (Fig. 8b, e; Table 3). Larvae could drift 73 (2004) and 106 days (2005) before reaching a nursery area (Table 3), and in 2006 drift trajectory indicated that larvae would not reach a nursery area.

Spawning area north of Nunivak Island

Drift in 2004, 2005, and 2010 was due north past the Norton Sound nursery so settlement of those larvae may have occurred in poor quality habitat (Fig. 8c, f). For 2002, 2006, 2007, and 2012 drift was due south to Nunivak Island, and 2016 drift track was to the northeast toward the coastline (Fig. 8c, f). Drift in 2002 showed a prolonged duration to reach nursery areas (98 days to reach Nunivak Island), indicating that larvae may have had to settle outside of nursery areas in unfavorable habitat (Fig. 8f; Table 3).

4. DISCUSSION

Results of this study indicate that variation in the distribution and density of YFS larvae in the inner domain of the eastern Bering Sea among warm and cold years may be explained by a

413 combination of temperature effects on the extent of the spawning area and timing of spawning,
414 and on the survival of eggs and larvae. IRI was a significant covariate in both the best-fit
415 presence-absence and larval density models, and was an indicator of temperature conditions, in
416 that sea-ice retreated earlier in warm conditions and later during cold conditions (Table 1). The
417 YFS commercial fishery most likely had little effect on the distribution of eggs and larvae in this
418 study because YFS are not an overfished species and total allowable catch is typically not caught
419 (pers. comm. Ingrid Spies, NOAA, Alaska Fisheries Science Center). Additionally, fishing
420 occurred in a similar area each year regardless of temperature condition (Spies et al., 2020). In
421 the southern region, the spatial extent of the predicted larval distribution varied with temperature
422 conditions. Larvae were widespread across that area during warm years and they were distributed
423 closer to shore in cold years. The difference in spatial distribution between temperature
424 conditions could be the result of changes in the extent of the spawning area as adults moved to
425 stay in preferred temperatures (1-7° C; Bartolino et al., 2011). Relatively warm bottom water
426 temperature caused the spawning area to expand to the west, and spawning area contracted to the
427 east when bottom water temperatures were cold. Previous studies showed that during both warm
428 and cold years, mature YFS females are found in the inner domain during the summer (Nichol et
429 al., 2019), and a majority of YFS spawning takes place in water < 30 m depth (Nichol, 1995).
430 Results here suggest that during warm conditions, the spawning area may expand westward
431 beyond 30 m depth because of favorable temperatures extending offshore. A previous study
432 showed that YFS adults moved northward in the eastern Bering Sea in response to warming
433 temperatures (Bartolino et al., 2011) suggesting that spawning YFS could follow warm water
434 offshore leading to an expansion of the spawning area. Regardless of temperature condition, the
435 highest density of larvae in the northern region was located between the coastline and 30 m

depth. The consistent distribution of larvae in the northern region among years may be due to less interannual variability in temperature in that area compared to the southern region (Stabeno et al., 2012a).

Temperature conditions altering the location of YFS spawning within the inner domain is supported by differences in the distribution of their eggs with bottom depth between warm and cold conditions. Currents in the inner domain are weak (Kinder and Schumacher, 1981; Stabeno et al., 2016) so egg distribution should show approximately where spawning occurred. During cold conditions, egg abundance was skewed toward shallow water (< 30 m depth), suggesting that spawning YFS adults avoided the relatively cold temperatures in deeper water and remained in warmer waters near shore. Egg abundance was similar among bottom depth intervals when relatively warm water occurred throughout the inner domain indicating a westward expansion of the spawning area during warm conditions. Expansion of the spawning area of Flathead Sole *Hippoglossoides elassodon* during warm conditions in the Bering Sea has also been observed (Porter and Ciannelli, 2018). It is acknowledged that in the present study, bottom water temperature measurements were taken earlier (June through July/early August, AFSC bottom trawl survey) than when eggs and larvae were collected (mid-August through September), so temperatures in the inner domain later in the summer may have been different than those shown in Figure 6. Temperatures measured during the bottom trawl survey were used because they were measured at the same time and location each year allowing consistent comparisons among years.

Results of this study suggest that not only can the location of YFS spawning be affected by temperature, the timing of spawning may vary between warm and cold conditions as well. The variability in the timing of spawning between temperature conditions could have resulted in the observed differences in larval density among warm and cold years. Ichthyoplankton surveys

were conducted at the same time of year, so if spawning were delayed during cold conditions fewer larvae would be present than would be present during warm conditions. Timing of spawning was not examined directly here because eggs were not sampled throughout the spawning season, that is, only eggs sampled in August and September were in common to all years. Earlier YFS spawning during warm conditions may be due to earlier seasonal gonadal development, and/or increase in the rate of gonadal development, resulting in earlier spawning migrations (Nichol et al., 2019). Additionally, migrations may begin sooner because of an earlier ice-edge retreat or preferred bottom temperatures (Nichol et al., 2019).

In addition to impacts on the spatial extent and timing of spawning, results of this study showed that temperature affected YFS larvae density. Density increased as near bottom temperature warmed to 10° C suggesting early life survival improved during warm years and may have contributed to larvae being more abundant during those years. Relatively warmer temperatures may be beneficial for YFS egg and larvae survival because temperatures colder than 4° C negatively affect survival of YFS eggs (Bakkala, 1981), and may also adversely affect survival of YFS larvae. Four degrees Celsius is near the lower temperature limit of survival for Yellowtail Flounder larvae, and Yellowtail Flounder larvae survival was highest when temperatures were relatively warm, between 8° and 14° C (Howell, 1980; Laurence and Howell, 1981) supporting that warm temperatures are favorable for early life stages of YFS. Increased YFS larvae density at warmer temperatures could also be related to earlier spawning during warm years.

Apparent from drift trajectories was that depending on spawning location and year, the time needed for larvae to reach nursery areas from spawning grounds could be longer than their estimated pelagic phase (30 to 60 days; Duffy-Anderson et al., 2015). The spawning areas north

and south of Nunivak Island had the most years that drift trajectories were longer than 60 days before reaching the shoreline or that the trajectory never reached shore during the drift period examined (Table 3). Environmental conditions (warm or cold year) during which the modeled drift period was long (> 60 days) were inconsistent, that is, an extended drift period did not consistently occur during only warm or cold conditions (Table 3). A potential consequence of a prolonged drift period to reach nursery areas is that larvae would have to settle before they arrived at a nursery, possibly in poor quality habitat. Early life survival is dependent upon reaching nurseries with suitable qualities such as the preferred substrate type and prey availability, and decreased juvenile growth and survival may result when settlement occurs outside of nursery areas.

YFS adults and juveniles in the eastern Bering Sea moved northward during warming ocean conditions (Bartolino et al., 2011). As the northern Bering Sea warms, increased abundance and wider distribution of YFS larvae in that area could occur and resemble the southern region during warm conditions. The northern region may not be as favorable for settlement of larvae in suitable habitat as in the south because larvae that hatch from the northern spawning areas can experience prolonged drift leading to settlement outside of nursery areas. The continued warming of the eastern Bering Sea may result in temperatures in shallow nearshore nursery areas increasing to the thermal limit of juvenile YFS negatively affecting their survival (Spies et al., 2020). Spatial variability of the quality of juvenile YFS habitat in the eastern Bering Sea and how that may affect juvenile growth and survival during warming ocean conditions requires further study.

The northward movement of fishes in the eastern Bering Sea due to warm conditions (e.g., Stevenson and Lauth, 2019) can alter the interactions between juvenile YFS and both their

505 predators and competing species. The predators of juvenile YFS are moving northward in
506 response to the eastern Bering Sea warming (Pacific Cod, *Gadus macrocephalus*; Stevenson and
507 Lauth, 2019). Cold pool extent limits the size of habitat available to YFS predators, and can
508 cause a concentration of predators in certain areas (Uchiyama et al., 2020) exposing YFS
509 juveniles to increased risk of predation. Northward shift in fish populations can also lead to
510 increased competition between species. For example, a warmer environment caused a northward
511 shift in juvenile Northern Rock Sole that increased their spatial overlap with juvenile YFS,
512 potentially increasing competition between these two species (Yeung and Cooper, 2020).
513 There is not a consistent trend between estimated recruitment of age-5 YFS and warm or cold
514 years (Spies et al., 2020) indicating the complex relationship between environmental drivers and
515 recruitment of this species. This study showed that changing environmental conditions affected
516 the spatial distribution of YFS larvae but how that may affect recruitment needs further study.
517 Success in reaching nurseries may play a role in recruitment variability in flatfishes (Bailey et.
518 al, 2008) suggesting that year class strength of YFS could be set at the late larval or juvenile
519 stage. Research related to the early life of YFS in the eastern Bering Sea (e.g., spatial variation in
520 the quality of juvenile nursery habitats) may identify mechanisms that affect recruitment during
521 changing climate conditions and aid in the effective management of this commercially important
522 species.
523

524 ACKNOWLEDGEMENTS
525 I thank A. Deary, L. Logerwell, L. Rogers, I. Spies, and C. Yeung for comments on early drafts
526 of the manuscript. This work was supported by the NOAA Ecosystems and Fisheries
527 Oceanography and Coordinated Investigations program and the North Pacific Climate Regimes

and Ecosystem Productivity program. This is research is contribution EcoFOCI-1010 to NOAA's Fisheries-Oceanography Coordinated Investigations. The findings and conclusions in the paper are those of the author and do not necessarily represent the views of the National Marine Fisheries Service. Reference to trade names does not imply endorsement by the National Marine Fisheries Service, NOAA.

CONFLICT OF INTEREST

The author has no conflict of interest to declare.

AUTHOR CONTRIBUTION

SMP conceived the project, acquired and analyzed the data, and drafted the manuscript.

DATA AVAILABILITY STATEMENT

The data that support the findings of this study are available from the corresponding author upon reasonable request.

544 REFERENCES

545 Bacheler, N.M., Bailey, K.M., Ciannelli, L., Bartolino, V., Chan, K.-S. (2009). Density
546 dependent, landscape, and climate effects on spawning distribution of walleye pollock
547 *Theragra chalcogramma*. *Marine Ecology Progress Series*, 391, 1–12.
548 doi:10.3354/meps08259
549
550 Bailey, K.M., Abookire, A.A., Duffy-Anderson J.T. (2008). Ocean transport paths for the early
551 life history stages of offshore-spawning flatfishes: a case study in the Gulf of Alaska. *Fish*
552 *and Fisheries*, 9, 44-66. doi:10.1111/J.1467-2979.2007.00268.X
553
554 Bakkala, R.G. (1981). Population characteristics and ecology of yellowfin sole. In D.W.
555 Hood and J.A. Calder (Eds.), *The Eastern Bering Sea shelf: Oceanography and resources*
556 (pp. 553-574). Volume 1. U.S. Dep. Commer., Natl. Oceanic Atmos. Admin., Mar. Poll.
557 Assess., U.S. Gov. Print Off., Washington, D.C.
558
559 Barbeaux, S.J., Hollowed, A.B. (2018). Ontogeny matters: Climate variability and effects on fish
560 distribution in the eastern Bering Sea. *Fisheries Oceanography*, 27, 1–15.
561 doi:10.1111/fog.12229
562
563 Bartolino, V., Ciannelli, L., Bacheler, N.M., Chan, K-S (2011). Ontogenetic and sex-specific
564 differences in density-dependent habitat selection of a marine fish population. *Ecology*, 92,
565 189-200. doi: 10.1890/09-1129.1
566

567 Ciannelli L., Bailey K., Olsen E.M. (2015). Evolutionary and ecological constraints of fish
568 spawning habitats. *ICES Journal of Marine Science*, 72, 285–296.
569 doi:10.1093/icesjms/fsu145
570
571 Coachman, L.K. (1986). Circulation, water masses, and fluxes on the southeastern Bering Sea
572 shelf. *Continental Shelf Research*, 5, 23-108. https://doi.org/10.1016/0278-4343(86)90011-7
573
574 Cooper, D.W., Duffy-Anderson, J.T., Norcross, B.L., Holladay, B.A., Stabeno, P.J. (2014).
575 Nursery areas of juvenile northern rock sole (*Lepidopsetta polyxystra*) in the eastern Bering
576 Sea in relation to hydrography and thermal regimes. *ICES Journal of Marine Science*, 71,
577 1683-1695. doi:10.1093/icesjms/fst210
578
579 Cooper, J. A., Chapleau, F. (1998). Monophyly and interrelationships of the family
580 Pleuronectidae (Pleuronectiformes), with a revised classification. *Fishery Bulletin*, 96, 686–
581 726.
582
583
584 Duffy-Anderson, J.T., Bailey, K.M., Cabral, H.N., Nakata, H., van der Veer, H.W., 2015. The
585 planktonic stages of flatfish: Physical and biological interactions in transport processes.
586 In R.N. Gibson, R.D.M. Nash, A.J. Geffen, and H.W. van der Veer (Eds.), *Flatfishes*
587 *Biology and Exploitation*, (pp. 132-171). West Susex: John Wiley & Sons, Ltd.
588 http://dx.doi.org/10.1002/9781118501153.ch6
589 ECODAAT ichthyoplankton database. NOAA, Alaska Fisheries Science Center, 7600 Sand
590 Point Way NE, Seattle, WA., 98115 USA. http://ecodaat.afsc.noaa.gov/

Environmental Systems Research Institute, Inc. (ESRI), 2018. *ArcGIS Release 10.7*. Redlands, CA.

Fox, C.J., O'Brien, C.M., Dickey-Collas, M., Nash, R.D.M. (2000). Patterns in the spawning of cod (*Gadus morhua* L.), sole (*Solea solea* L.) and plaice (*Pleuronectes platessa* L.) in the Irish Sea as determined by generalized additive modeling. *Fisheries Oceanography*, 9, 33-49. http://dx.doi.org/10.1046/j.1365-2419.2000.00120.x

Howell, W.H. (1980). Temperature effects on growth and yolk utilization in yellowtail flounder, *Limanda ferruginea*, yolk-sac larvae. *Fishery Bulletin, U.S.*, 78, 731-739.

Kinder, T.H., Schumacher, J.D. (1981). Hydrographic structure over the continental shelf of the southeastern Bering Sea. In D.W. Hood and J.A. Calder (Eds.), *The Eastern Bering Sea shelf: Oceanography and resources* (pp. 31-52). Volume 1. U.S. Dep. Commer., Natl. Oceanic Atmos. Admin., Mar. Poll. Assess., U.S. Gov. Print Off., Washington, D.C.

Kotwicki, S., Lauth, R.R. (2013). Detecting temporal trends and environmentally-driven changes in the spatial distribution of bottom fishes and crabs on the eastern Bering Sea shelf. *Deep-Sea Research II*, 94, 231-243. https://doi.org/10.1016/j.dsr2.2013.03.017

Laurence, G.C., Howell, W.H. (1981). Embryology and influence of temperature and salinity on

614 early development and survival of Yellowtail Flounder *Limanda ferruginea*. *Marine*
615 *Ecology Progress Series*, 6, 11-18.
616
617 Leggett, W.C. (1985). The role of migrations in the life history evolution of fish. In M.A.R.
618 Rankin (Ed.), *Migration: Mechanisms and Adaptive Significance* (pp. 277-295).
619 Contributions to Marine Science, Supplement 27, Marine Science Institute, University of
620 Texas, Austin.
621
622 Matarese, A.C., Blood, D.M., Picquelle, S.J., Benson, J.L. (2003). *Atlas of abundance and*
623 *distribution patterns of ichthyoplankton from the northeast Pacific Ocean and Bering Sea*
624 *ecosystems based on researched conducted by the Alaska Fisheries Science Center (1972-*
625 *1996)*. U.S. Dep. Commer., NOAA Prof. Paper NMFS-1.
626
627 Nichol, D.G. (1995). Spawning and maturation of female yellowfin sole in the eastern
628 Bering Sea. In *Proceedings of the International Symposium on North Pacific Flatfish* (p.
629 35-50). Alaska Sea Grant Program Report No. 95-04, University of Alaska Fairbanks.
630
631 Nichol, D.G., Acuna, E.I. (2001). Annual and batch fecundities of yellowfin sole, *Limanda*
632 *aspera*, in the eastern Bering Sea. *Fishery Bulletin, U.S.*, 99, 108-122.
633
634 Nichol, D.G., Kotwicki, S., Wilderbuer, T.K., Lauth, R.R., Ianelli, J.N. (2019). Availability of
635 yellowfin sole *Limanda aspera* to the eastern Bering Sea trawl survey and its effect on
636 estimates of survey biomass. *Fisheries Research*, 211, 319-330.

https://doi.org/10.1016/j.fishres.2018.11.017

Porter, S.M., Ciannelli, L. (2018). Effect of temperature on Flathead Sole (*Hippoglossoides elassodon*) spawning in the southeastern Bering Sea during warm and cold years. *Journal of Sea Research*, 141, 26-36. https://doi.org/10.1016/j.seares.2018.08.003

Potts, J.M., Elith, J. (2006). Comparing species abundance models. *Ecological Modelling*, 199, 153-163. https://doi.org/10.1016/j.ecolmodel.2006.05.025

R Core Team (2019). *R: A Language and Environment for Statistical Computing*. R Foundation for Statistical Computing, Vienna, Austria.

Smith, W.G., Sibunka, J.D., Wells, A. (1978). Diel movements of larval yellowtail flounder, *Limanda ferruginea,* determined from discrete depth sampling. *Fishery Bulletin, U.S.*, 76, 167-178.

Spies, I, Wilderbuer, T.K., Nichol, D.G., Ianelli, J. (2019). Assessment of the yellowfin sole stock in the Bering Sea and Aleutian Islands. In *Stock Assessment and Fishery Evalution Report for the Groundfish Resources of the Bering Sea/Aleutian Islands Regions* (pp. 1-88). North Pacific Fisheries Management Council, 1007 West Third, Suite 400, Anchorage, Alaska 99501.

Spies, I, Haehn, R, Siddon, E., Conner, J., Britt, L, Ianelli, J. (2020). Assessment of the

660 yellowfin sole stock in the Bering Sea and Aleutian Islands. In *Stock Assessment and*
661 *Fishery Evalution Report for the Groundfish Resources of the Bering Sea/Aleutian Islands*
662 *Regions* (pp. 1-97). North Pacific Fisheries Management Council, 1007 West Third, Suite
663 400, Anchorage, Alaska 99501.
664
665 Stabeno, P.J., Bond, N.A., Kachel, N.B., Salo, S.A., Schumacher, J.D. (2001). On the temporal
666 variability of the physical environment over the south-eastern Bering Sea. *Fisheries*
667 *Oceanography*, 10, 81-98. https://doi.org/10.1046/j.1365-2419.2001.00157.x
668
669 Stabeno, P.J., Napp, J., Mordy, C., Whitledge, T. (2010). Factors influencing physical structure
670 and lower trophic levels of the eastern Bering Sea shelf in 2005: sea ice, tides and winds.
671 *Progress in Oceanography*, 85 (3–4), 180–196. doi:10.1016/j.pocean.2010.02.010
672
673 Stabeno, P.J., Farley, E.V., Kachel, N.B., Moore, S., Mordy, C.W., Napp, J.M., Overland, J.E.,
674 Pinchuk, A.I., Sigler, M.F. (2012a). A comparison of the physics of the northern and
675 southern shelves of the eastern Bering Sea and some implications for the ecosystem. *Deep-*
676 *Sea Research II*, 65-70, 14-30. doi:10.1016/j.dsr2.2012.02.019
677
678 Stabeno, P.J., Kachel, N.B., Moore, S.E., Napp, J.M., Sigler, M., Yamaguchi, A., Zerbini, A.N.
679 (2012b). Comparison of warm and cold years on the southeastern Bering Sea shelf and some
680 implications for the ecosystem. *Deep-Sea Research II*, 65-70, 31-45.
681 doi:10.1016/j.dsr2.2012.02.020
682

683 Stabeno, P.J., Danielson, S.L., Kachel, D.G., Kachel, N.B, Mordy, C.W. (2016). Currents and
684 transport on the Eastern Bering Sea shelf: An integration of over 20 years of data. *Deep-Sea*
685 *Research II*, 134, 13-29. https://doi.org/10.1016/j.dsr2.2016.05.010
686
687 Stabeno, P.J., Duffy-Anderson, J.T., Eisner, L.B., Farley, E.V., Heintz, R.A., Mordy, C.W.
688 (2017). Return of warm conditions in the southeastern Bering Sea: Physics to fluorescence.
689 *PLoS ONE*, 12, e0185464. https://doi.org/10.1371/journal.pone.0185464
690
691 Stabeno, P.J., Bell, S.W., Bond, N.A., Kimmel, D.G., Mordy, C.W., Sullivan, M.E. (2019).
692 Distributed Biological Observatory Region 1: Physics, chemistry and plankton in the
693 northern Bering Sea. *Deep-Sea Research II*, 162, 8-21.
694 https://doi.org/10.1016/j.dsr2.2018.11.006
695
696 Stabeno, P.J., Bell, S.W. (2019). Extreme conditions in the Bering Sea (2017–2018): Record-
697 breaking low sea-ice extent. *Geophysical Research Letters*, 46, 8952-8959.
698 https://doi.org/10.1029/2019GL083816
699
700 Stevenson, D.E., Lauth, R.R. (2019). Bottom trawl surveys in the northern Bering Sea indicate
701 recent shifts in the distribution of marine species. *Polar Biology*, 42, 407-421.
702 https://doi.org/10.1007/s00300-018-2431-1
703
704 Uchiyama, T., Mueter, F.J., Kruse, G.H. (2020). Multispecies biomass dynamics models reveal
705 effects of ocean temperature on predation of juvenile pollock in the eastern Bering Sea.

706 *Fisheries Oceanography*, 29, 10-22. doi: 10.1111/fog.12433
707
708 Wakabayashi, K. (1989). Studies on the fishery biology of yellowfin sole in the eastern Bering
709 Sea. [In Japanese, English Summary] *Bulletin. Far Seas Fisheries Research Laboratory*, 26,
710 21-152.
711
712 Waldron, K. D. (1981). Ichthyoplankton. In D.W. Hood and J.A. Calder (Eds.), *The Eastern*
713 *Bering Sea shelf: Oceanography and resources* (pp. 471-493). Volume 1. U.S. Dep.
714 Commer., Natl. Oceanic Atmos. Admin., Mar. Poll. Assess., U.S. Gov. Print Off.,
715 Washington, D.C.
716
717 Wilderbuer, T.K., Walters, G.E., Bakkala, R.G. (1992). Yellowfin sole, *Pleuronectes asper*, of
718 the eastern Bering Sea: biological characteristics, history of exploitation, and management.
719 *Marine Fisheries Review*, 54, 1-18.
720
721 Wilderbuer, T.K., Nichol, D.G., Ianelli, J. (2018). Assessment of the yellowfin sole stock in the
722 Bering Sea and Aleutian Islands. In *Stock Assessment and Fishery Evalution Report*
723 *for the Groundfish Resources of the Bering Sea/Aleutian Islands Regions* (pp. 1-84). North
724 Pacific Fisheries Management Council, 1007 West Third, Suite 400, Anchorage, Alaska
725 99501.
726
727 Wood, S.N. (2006). *Generalized additive models: an introduction with R* (p. 392). Boca Raton,
728 Florida: Chapman and Hill/CRC.

Yeung, C., Yang, M-S. (2017). Habitat quality of the coastal southeastern Bering Sea for juvenile flatfishes from the relationships between diet, body condition and prey availability. *Journal of Sea Research*, 119, 17-27. doi:10.1016/j.seares.2016.10.002

Yeung, C., Yang, M-S. (2018). Spatial variation in habitat quality for juvenile flatfish in the southeastern Bering Sea and its implications for productivity in a warming ecosystem. *Journal of Sea Research*, 139, 62-72. http://dx.doi.org/10.1016/j.seares.2018.06.005

Yeung, C., Cooper D.W. (2020). Contrasting the variability in spatial distribution of two juvenile flatfishes in relation to thermal stanzas in the eastern Bering Sea. *ICES Journal of Marine Science*, 77, 953-963. doi:10.1093/icesjms/fsz180

744 FIGURE LEGENDS

745 Figure 1. The eastern Bering Sea shelf. The inner domain is located between the coastline and
746 depths ≤ 50 m. The middle domain is 50 < depths ≤ 100 m.

747

748 Figure 2. Observed Yellowfin Sole larvae density (number/10 m^2) for 2002, 2004-2007, 2010,
749 2012, and 2016 used to model the effect of the timing of sea-ice edge retreat, spatial extent of
750 water ≤ 0° C, and water temperature on the spatial distribution of larvae in the inner domain of
751 the eastern Bering Sea. For 2016 in the southern region, stations showing no larvae present (X)
752 were occupied in May and on June 1 (beginning of the Yellowfin Sole spawning season).

753

754 Figure 3. Partial effects for covariates included in the spatially variable coefficient generalized
755 additive model for Yellowfin Sole larvae presence/absence shown in Table 2, equation 3. a.
756 Effect of day of year. Rug on x-axis represents data. Grey area indicates 95% confidence
757 interval. b. Effect of location. Positive values are yellow, and negative values are orange and red.
758 c. Effect of near bottom temperature. Rug on x-axis represents data. Grey area indicates 95%
759 confidence interval. d. Spatially variable effect of ice retreat index. Positive values are yellow,
760 and negative values are orange and red. e. Effect of year as a factor. Warm years were 2002,
761 2004, 2005, and 2016; average year was 2006; cold years were 2007, 2010, and 2012. Dashed
762 lines show standard error.

763

764 Figure 4. Partial effects for covariates included in the spatially variable coefficient generalized
765 additive model for Yellowfin Sole larvae density shown in Table 2, equation 4. a. Effect of day
766 of year. Rug on x-axis represents data. Grey area indicates 95% confidence interval. b. Effect of

location. Positive values are yellow, and negative values are orange and red. c. Effect of near bottom temperature. Rug on x-axis represents data. Grey area indicates 95% confidence interval. d. Spatially variable effect of ice retreat index. Positive values are yellow, and negative values are orange and red. e. Spatially variable effect of ratio of area covered by bottom water ≤ 0° C to total bottom trawl survey area. Positive values are yellow, and negative values are orange and red. f. Effect of year as a factor. Warm years were 2002, 2004, 2005, and 2016; average year was 2006; cold years were 2007, 2010, and 2012. Dashed lines show standard error.

Figure 5. Predicted density of Yellowfin Sole larvae (ln(number/10 m^2)) in the inner domain of the eastern Bering Sea for years 2002, 2004-2007, 2010, 2012, and 2016.

Figure 6. Bottom water temperature measured during the Alaska Fisheries Science Center annual summer bottom trawl survey (June ~ late July or early August) in the southeastern Bering Sea for 2002, 2004-2007, 2010, 2012, and 2016.

Figure 7. Distribution of *Limanda* sp. eggs by bottom depth interval and temperature category in the southern region of the study area. Not-cold category included years 2002, 2004-2006, 2016, and cold category had 2007, 2010, and 2012. Mean ± standard error is shown.

Figure 8. Drift trajectories starting from near the center of three Yellowfin Sole spawning areas (Bristol Bay, South of Nunivak Island, and North of Nunivak Island, redrawn from Figure 16, Wakabayashi, 1989; star indicates starting point of drift) in the eastern Bering Sea study area for

789 2002, 2004-2007, 2010, 2012, and 2016. Drift period for each year was from June 1 to October
790 6.

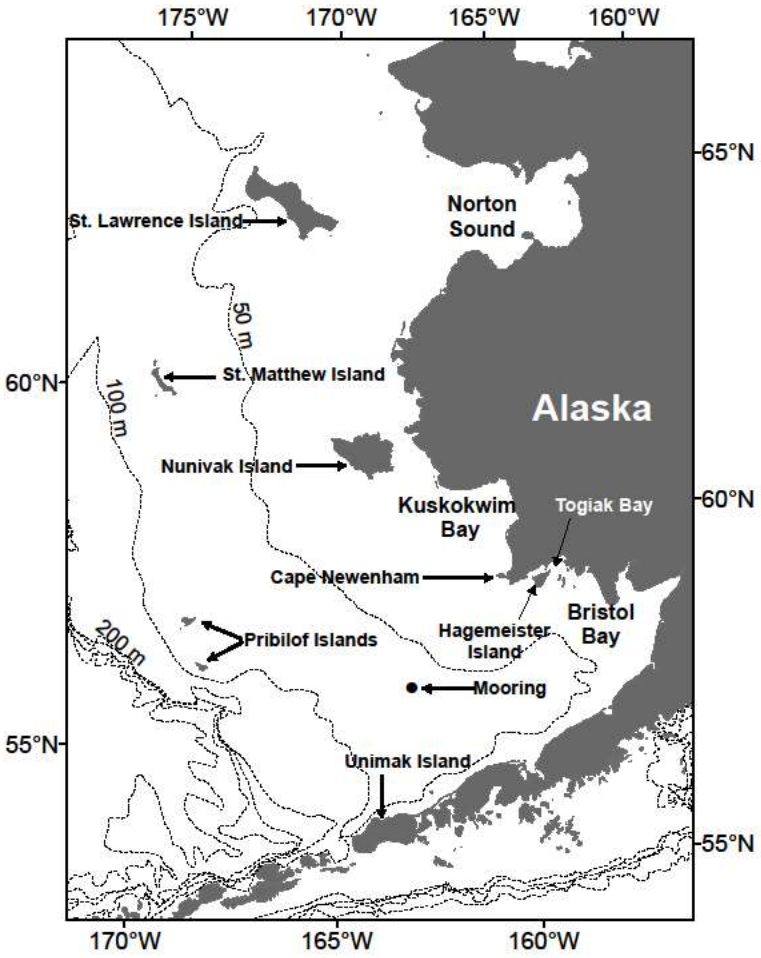

791

792 Figure 1

793

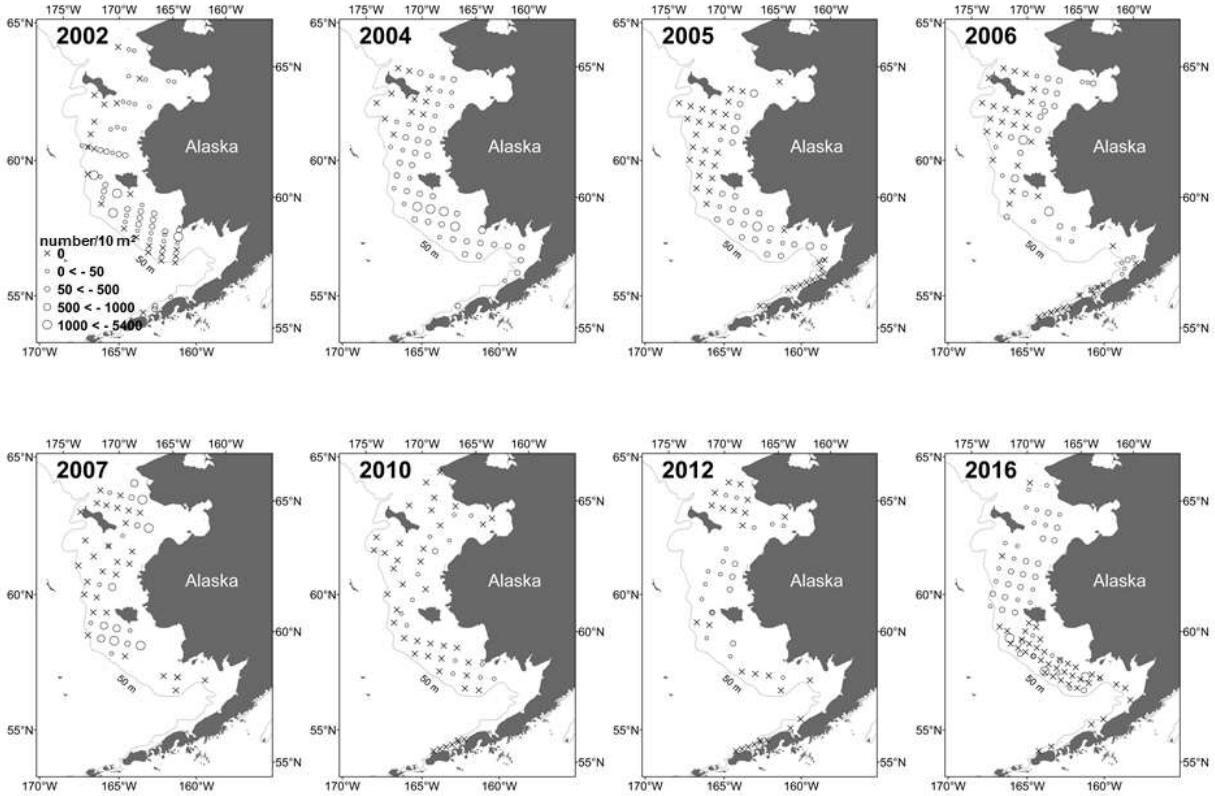

794

795 Figure 2

796

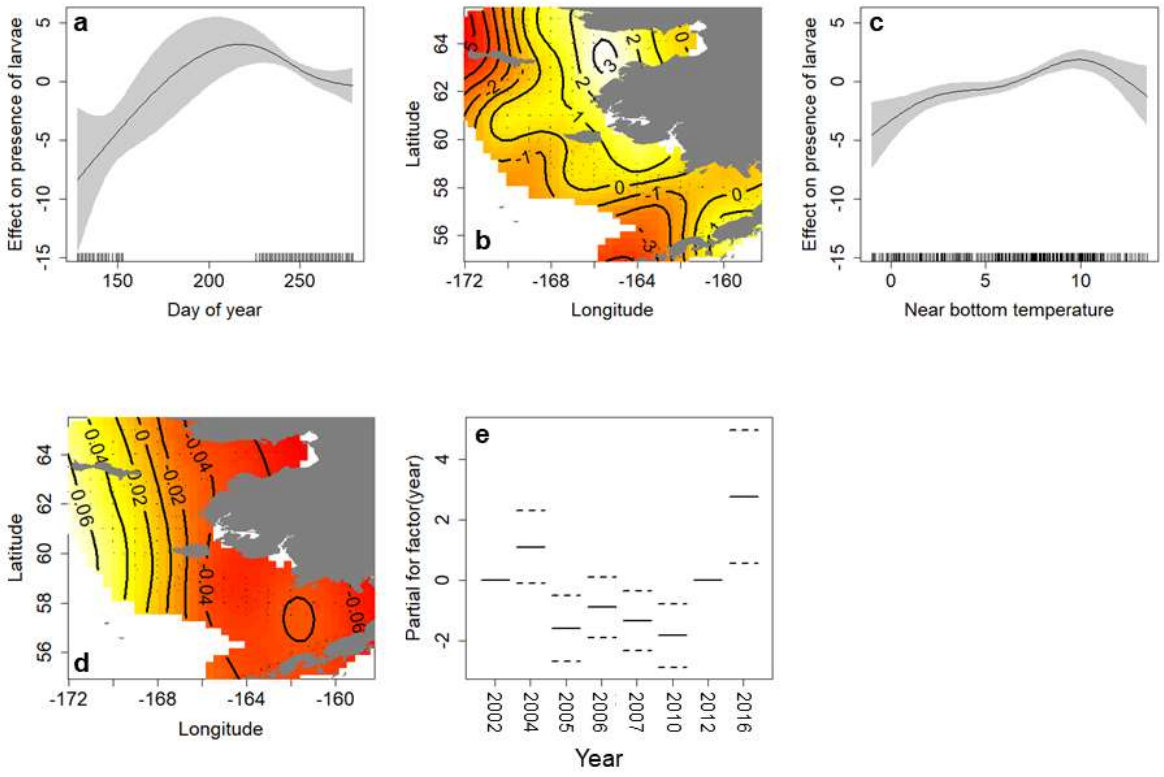

797

798 Figure 3

799

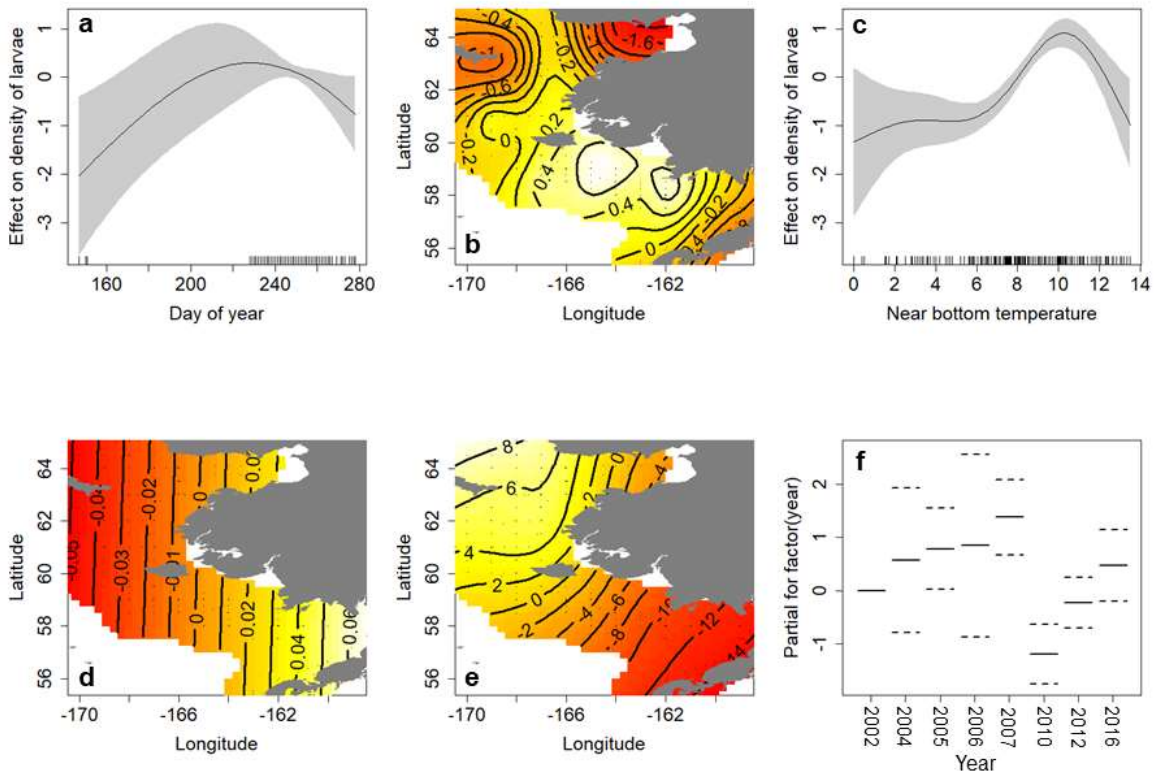

800

801 Figure 4

802

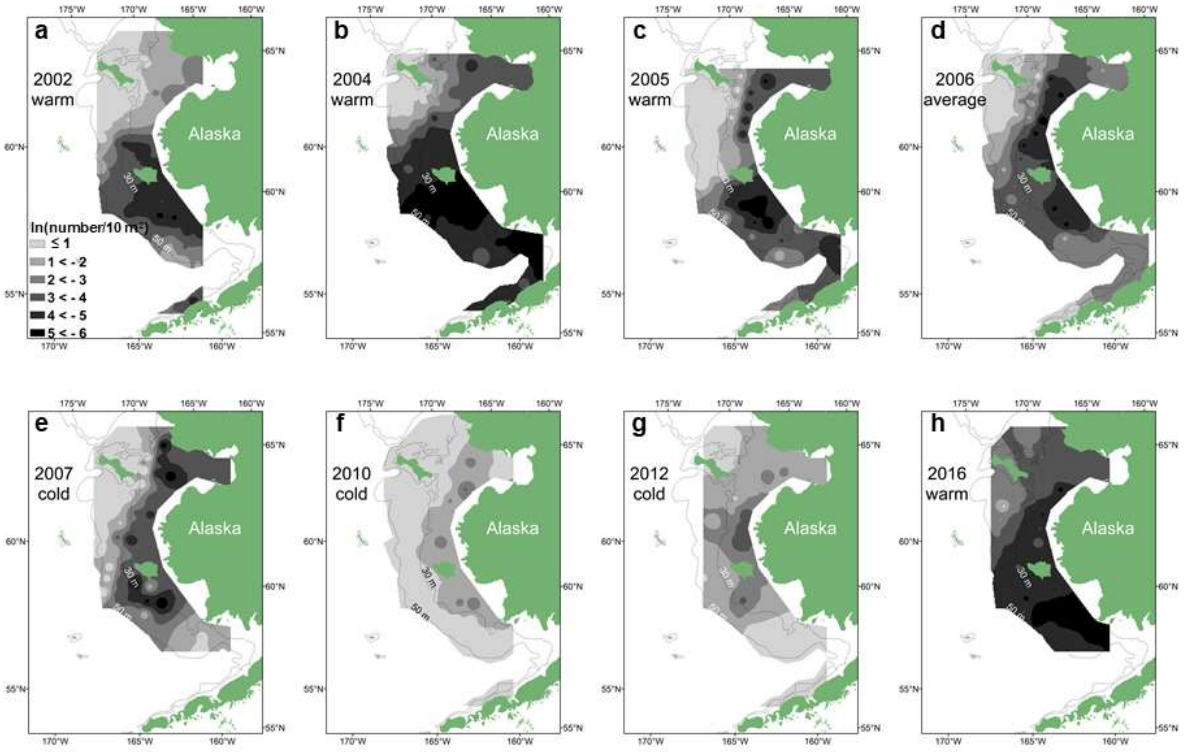

803

804 Figure 5

805

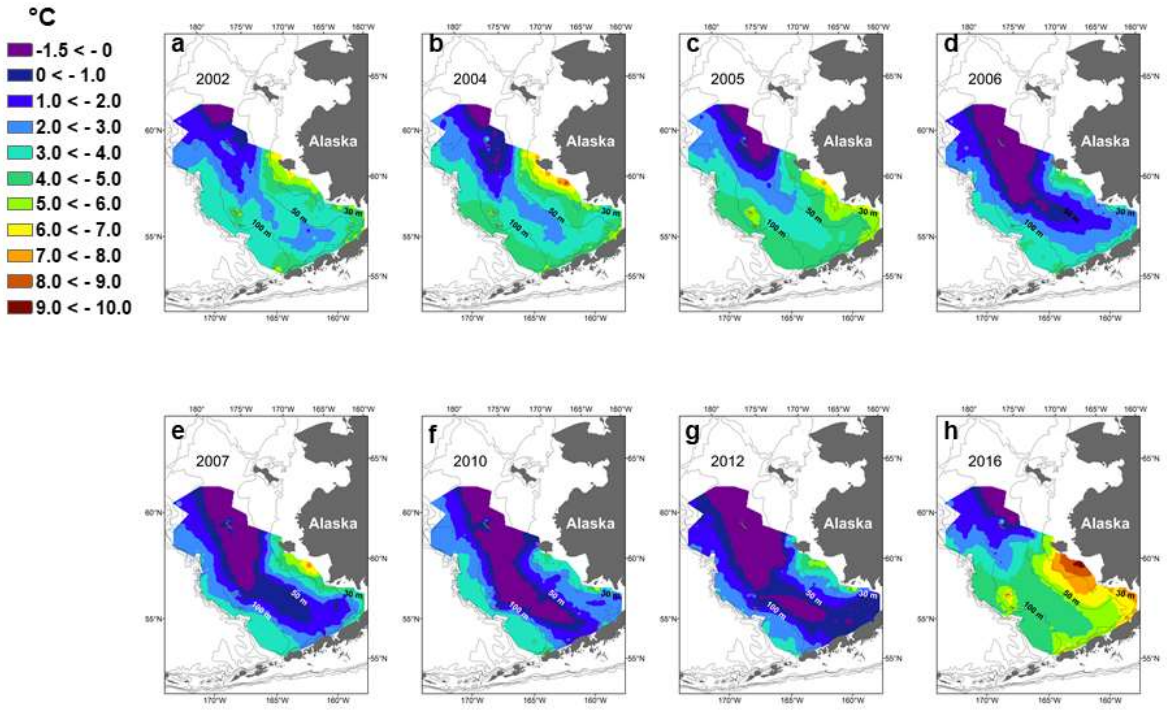

806

807 Figure 6

808

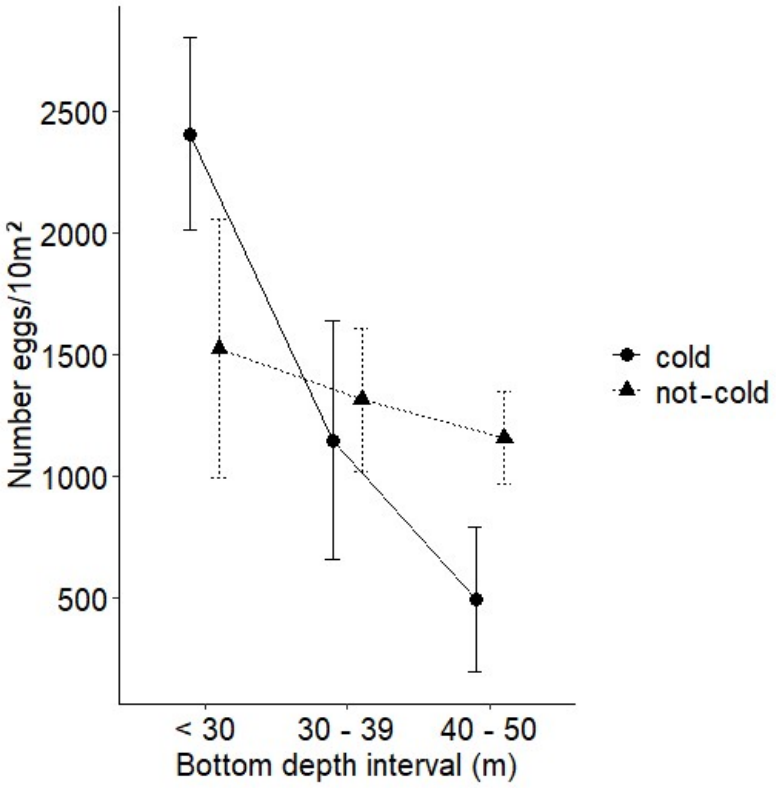

809

810 Figure 7

811

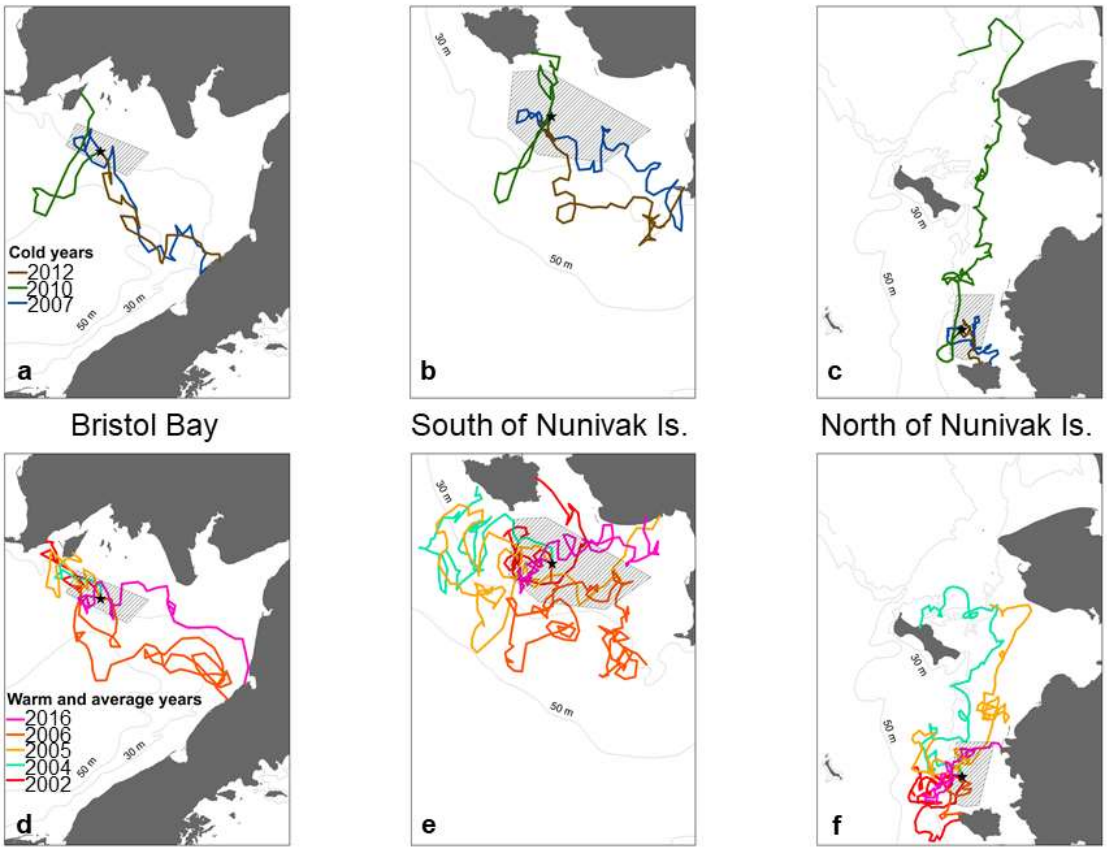

812

813 Figure 8

Table 1. Survey years in the eastern Bering Sea used to model the spatial variation of Yellowfin Sole larvae during warm, cold, and average years.

			Southern Region (< 60° N)					Northern Region (≥ 60° N)				
Year	IRI[†]	RA0C[‡]	n	Temperature[§]	Day of year[¶]	Median DOY	Catch/10m^2 [††]	n	Temperature	Day of year	Median DOY	Catch/10m^2
2002	0	0.0322	41	8.5 ± 2.5	134-262	244	287.56 ± 861.30	31	5.7 ± 2.9	262-279	272	92.92 ± 338.40
2004	9	0.0208	27	9.5 ± 2.1	228-247	234	522.68 ± 995.60	35	6.6 ± 3.9	255-272	261	48.97 ± 67.59
2005	0	0.0492	37	7.5 ± 3.1	131-278	230	147.99 ± 235.32	28	5.7 ± 3.5	260-276	269	63.49 ± 171.69
2006	13	0.1824	39	8.1 ± 2.9	135-263	254	77.27 ± 230.56	38	4.8 ± 3.5	246-261	251	101.47 ± 199.00
2007	28	0.1696	17	6.5 ± 2.6	228-276	238	287.44 ± 477.39	33	5.4 ± 3.5	256-273	263	258.01 ± 956.24
2010	37	0.2468	29	6.1 ± 2.8	128-257	239	1.35 ± 2.58	27	4.7 ± 4.3	242-276	264	6.92 ± 16.77
2012	46	0.2956	21	4.7 ± 2.9	139-267	235	9.14 ± 27.00	25	4.9 ± 3.0	254-267	259	27.88 ± 63.00
2016	0	0.0380	52	6.1 ± 1.7	140-253	149	109.74 ± 374.98	32	6.3 ± 4.3	240-255	246	66.50 ± 69.86

[†]ice retreat index
[‡]ratio of the area of bottom water ≤ 0°C to total AFSC bottom trawl survey area
[§]near bottom temperature, approximately 10 m off bottom; mean ± standard deviation
[¶]interval of days that samples were taken. For all years, only one sample was taken in June and there were no samples taken in July.
[††]mean ± standard deviation

Table 2. Generalized additive models to analyze the variation of the presence/absence and density of Yellowfin Sole larvae in the eastern Bering Sea during warm, cold, and average years. Best-fit models as determined by AIC value are shown.

	Covariates									
Spatially invariant model	s[§] (t[¶])	s(ϕ, λ) [‡‡]	s(d[§§])	yr[¶¶]	s(IRI) [†††]	s(RA0C) [‡‡‡]	s(ϕ, λ)IRI$_{(\phi, \lambda)}$	s(ϕ, λ)RA0C$_{(\phi, \lambda)}$	AIC	R^2
1[†]	1.000[††]	15.501	2.739	factor	-	-	NA	NA	417.60	0.51
2[‡]	3.793	15.286	3.768	factor	-	-	NA	NA	885.05	0.47
Spatially variable coefficient model										
3[†]	3.956	18.225	3.075	factor	NA	NA	6.914	-	408.18	0.55
4[‡]	3.821	14.181	2.232	factor	NA	NA	3.00	5.632	877.83	0.49

[†]presence/absence model. Numbers refer to equations 1 and 3 in Materials and Methods, 2.2 Generalized additive models

[‡]density model. Numbers refer to equations 2 and 4 in Materials and Methods, 2.2 Generalized additive models

[§]nonparametric smoothing function

[¶]near bottom temperature

[††]estimated degrees of freedom

[‡‡]location (latitude, longitude)

[§§]day of year

[¶¶]year

[†††]ice retreat index

[‡‡‡]ratio of area covered by bottom water ≤ 0°C to AFSC bottom trawl survey area

848

849 - = not included in final model as determined by AIC value

Table 3. Predicted number of days from June 1 to October 6 that a particle near the sea surface drifted from near the center of one of three YFS spawning areas before reaching the Alaskan shoreline (Ocean Surface Currents Simulations model, oceanview.pfeg.noaa.gov/oscurs; Fig. 8). For each year, drift began at the same location within each spawning area.

Year	Bristol Bay spawning area (days)	South Nunivak spawning area (days)	North Nunivak spawning area (days)
2002	17	54	98
2004	8	73	117
2005	22	106	Offshore
2006	66	Offshore†	25
2007	39	64	57
2010	22	40	Offshore
2012	31	56	20
2016	42	68	53

†drift trajectory never reached the shoreline during the drift period examined